

Spatially Constrained Spectral Clustering Algorithms for Region Delineation

Shuai Yuan¹ · Pang-Ning Tan¹ · Kendra Spence Cheruvellil² · Sarah M. Collins³ · Patricia A. Soranno³

Received: date / Accepted: date

Abstract Regionalization is the task of dividing up a landscape into homogeneous patches with similar properties. Although this task has a wide range of applications, it has two notable challenges. First, it is assumed that the resulting regions are both homogeneous and spatially contiguous. Second, it is well-recognized that landscapes are hierarchical such that fine-scale regions are nested wholly within broader-scale regions. To address these two challenges, first, we develop a spatially constrained spectral clustering framework for region delineation that incorporates the tradeoff between region homogeneity and spatial contiguity. The framework uses a flexible, truncated exponential kernel to represent the spatial contiguity constraints, which is integrated with the landscape feature similarity matrix for region delineation. To address the second challenge, we extend the framework to create fine-scale regions that are nested within broader-scaled regions using a greedy, recursive bisection approach. We present a case study of a terrestrial ecology data set in the United States that compares the proposed framework with several baseline methods for regionalization. Experimental results suggest that the proposed framework for regionalization outperforms the baseline methods, especially in terms of balancing region contiguity and homogeneity, as well as creating regions of more similar size, which is often a desired trait of regions.

Keywords Constrained spectral clustering · Regionalization · hierarchical clustering

1.Dept of Comp Science and Engr, Michigan State University
2.Dept of Fisheries and Wildlife & Lyman Briggs College, Michigan State University
3.Dept of Fisheries and Wildlife, Michigan State University

1 Introduction

A regionalization framework delineates the geographical landscape into spatially contiguous, homogeneous units known as regions or zones. Regionalizations are important because they provide the spatial framework used in many disciplines, including landscape ecology, environmental science, and economics, as well as for applications such as public policy and natural resources management [9,28,15,30]. For example, the hierarchical system of hydrologic units described in [41] provides a standardized regionalization framework that has been widely used in water resource and land use studies [14]. Abell et al. [1] have also developed a global biogeographic regionalization framework that serves as a useful tool for studying biodiversity in freshwater systems and for conservation planning efforts.

McMahon et al. [31] divide existing multivariate regionalization methods into two categories, qualitative and quantitative. For qualitative methods, regions with similar landscape characteristics are delineated by experts from multiple maps of different geographic features using manual visual interpretation [3,34]. For quantitative methods, clustering approaches such as k-means and hierarchical clustering [19,18,22] are used to partition the geographical area into smaller regions. Although quantitative clustering approaches provide a more systematic and reproducible way to identify regions compared to qualitative approaches, one potential limitation of existing clustering methods is that the regions created may not be spatially contiguous. Region contiguity is a desirable criterion for many applications that treat regions as individual entities for purposes including research, policy, and management (e.g., site-specific management in precision agriculture [27]). Therefore, alternative methods are needed that can effectively clus-

ter similar areas based on multiple mapped variables, but have the added constraint of being spatially contiguous.

In the preliminary version of this work [56], we presented a spatially constrained spectral clustering framework that uses a truncated exponential kernel [24] to produce spatially contiguous and homogeneous regions [23, 8, 43, 51]. In this paper, we extend the formulation to create hierarchical regions, where fine-scaled regions can be nested within broad-scale regions. Creating such nested regions is extremely useful for many applications because hierarchical structure is often held up as a fundamental feature of both the natural world and complex systems (as reviewed in [54]). In fact, the world's biomes and ecological regions have often been delineated in a nested hierarchical structure [4, 1]. Constrained versions of hierarchical clustering techniques [33] such as single-link [26], complete-link [37], UPGMA [25, 39], and Ward's method [20, 53] have often been used to create such nested regions. However, as will be shown in this study, the regions generated by such methods tend to be highly imbalanced in terms of their sizes, and thus, are not as suitable for many applications, including resource planning and management.

We use a recursive bisection approach to extend our formulation in [56] to hierarchical clustering. Our top-down approach for creating nested regions is different from the bottom-up approach commonly used by existing methods [20, 37, 25, 39, 53]. Using three criteria for region evaluation—landscape homogeneity, region contiguity, and region size—our experimental results suggest that the proposed framework outperforms three other constrained hierarchical clustering methods in 2 out of the 3 criteria. For example, it consistently produces regions that are more homogeneous and balanced in region size compared to the spatially constrained complete-link [37] and UPGMA [25, 39] algorithms. Our proposed algorithm also outperforms the constrained version of Ward's method [53] in terms of producing regions that are spatially contiguous and approximately uniform in size. Finally, although the spatially constrained single link method [26] is also capable of producing regions that are homogeneous and contiguous, it tends to create one or two very large regions that cover the majority of the landscape area. An ad-hoc parameter for maximum region size is needed by the spatially constrained single link method to prevent the formation of such large regions [38]. Tuning this parameter is cumbersome as it must be done at every level of the hierarchy since the maximum region size depends on the number of regions. Our proposed hierarchical method does not have such a problem because its objective function, which is based on the normalized cut criterion [42]

used in spectral clustering, is inherently biased towards producing more uniformly-sized clusters.

The remainder of this paper is organized as follows. Section 2 reviews previous work on the development of regionalization frameworks, constrained clustering, and hierarchical clustering methods. Section 3 formalizes the region delineation problem and presents an overview of spectral clustering. Section 4 describes the different ways in which spatial constraints can be incorporated into the spectral clustering framework. It also presents the partitional and hierarchical implementations of our proposed spatially constrained spectral clustering framework. Section 5 describes the application of spatially constrained spectral clustering algorithms to the region delineation problem. Section 6 concludes with a summary of the results of this study.

2 Related Work

Region delineation has traditionally been studied as a spatial clustering [17] problem. Duque et al. [14] classified the existing data-driven approaches into two categories. The first category does not require explicit representation and incorporation of spatial constraints into the clustering procedure. Instead, the constraints are satisfied by post-processing the clusters or optimizing other related criteria. For example, Openshaw [35] applied a conventional clustering method followed by a cluster refinement step to split clusters that contained geographically disconnected patches. The second category of methods explicitly incorporates spatial constraints into the clustering algorithm [14]. Examples of such methods include adapted hierarchical clustering, exact optimization methods, and graph theory based methods. This second category also encompasses the constrained clustering methods [2, 50, 12] developed in the fields of data mining and machine learning.

Constrained clustering [6, 50] is a semi-supervised learning approach that uses the domain information provided by users to improve clustering results. The domain information is typically provided as must-link (ML) and cannot-link (CL) constraints to be satisfied by the clustering solution. ML constraints restrict the pairs of data points that must be assigned to the same cluster, whereas CL constraints specify the pairs of points that must be assigned to different clusters. For example, Kamvar et al. [23] uses the ML and CL constraints to define the affinity matrix of the data. Shi et al. [43] proposed a constrained co-clustering method that considers both the similarity of features as well as the ML and CL constraints. All of these methods were designed to manipulate the graph Laplacian matrix using the domain constraints available. There has also

been growing interest in developing constrained-based approaches for spectral clustering [23, 8, 43, 51, 11]. For example, De Bie et al. [7] developed an approach that restricts the eigenspace for which the cluster membership vector is projected. Wang and Davison [51] proposed a constrained spectral clustering method that considers real-valued constraints and imposed a threshold on the minimum amount of constraints that must be satisfied by the feasible solution. However, none of these constrained spectral clustering methods were designed for the region delineation problem. The framework presented in our previous paper [56, 10] employs a Hadamard product to combine the feature similarity matrix with spatial contiguity constraints, which is similar to the approach used in Craddock et al. [11] for generating an ROI atlas of the human brain using fMRI data. However, unlike the approach used in [11], we consider a truncated exponential kernel to relax the spatial neighborhood constraints and perform extensive experiments comparing the framework to various constrained spectral clustering algorithms.

Current constrained spectral clustering algorithms have also focused primarily on partitioning clustering. They require the number of clusters to be specified *a priori*. In contrast, hierarchical methods generate a nested set of clustering for every possible number of clusters. The hierarchy of clusters, also known as a dendrogram, can be created either in a top-down (i.e., divisive hierarchical clustering) or bottom-up (i.e., agglomerative hierarchical clustering) fashion [49, 22, 21]. Some of the widely used agglomerative hierarchical clustering algorithms include single link [20], complete link [37], group average (UPGMA) [25, 39], and Ward’s method [22, 53] whereas examples of divisive hierarchical clustering algorithms include minimum spanning tree [16] and bisecting k-means [40]. Current approaches for creating nested regions are mostly based on different variations of agglomerative hierarchical clustering. Each of these variations has its own strengths and limitations [33]. For example, the single-link method can identify irregular shaped clusters but is highly sensitive to noise [49]. In contrast, the Ward’s method can minimize the cluster variance but is susceptible to the inversion problem [33]. Unfortunately, many of these agglomerative methods can produce highly imbalanced sizes of regions, which is not desirable for many applications [5].

3 Preliminaries

This section formalizes region delineation as a constrained clustering problem and presents a brief overview of spectral clustering and its constrained-based methods.

3.1 Region Delineation as Constrained Clustering Problem

Consider a data set $\mathcal{D} = \{(\mathbf{x}_i, \mathbf{s}_i)\}_{i=1}^N$, where $\mathbf{x}_i \in \mathbb{R}^d$ is a d -dimensional vector of landscape features associated with the geo-referenced spatial unit $\mathbf{s}_i \in \mathbb{R}^2$. Let $\mathcal{R} = \{1, 2, \dots, k\}$ denote the set of region identifiers, where k is the number of regions, and $\mathcal{C} = \{(\mathbf{s}_i, \mathbf{s}_j, \mathbf{C}_{ij})\}$ denote the set of spatial constraints. For region delineation, we consider only ML constraints and represent them using a constraint matrix \mathbf{C} defined as follows:

$$\mathbf{C}_{ij} = \begin{cases} 1 & \text{if } \mathbf{s}_i \text{ and } \mathbf{s}_j \text{ are spatially adjacent,} \\ 0 & \text{otherwise.} \end{cases} \quad (1)$$

The goal of region delineation is to learn a partition function \mathcal{V} that maps each spatial unit \mathbf{s}_i to its corresponding region identifier $r_i \in \mathcal{R}$ in such a way that (1) maximizes the similarity between the spatial units in each region and (2) minimizes the constraint violations in the set \mathcal{C} .

3.2 Spectral Clustering

Spectral clustering is a class of partitioning clustering algorithms that relies on the eigen-decomposition of an input affinity (similarity) matrix \mathbf{S} to determine the underlying clusters of the data set. Let $\{\mathbf{x}_1, \mathbf{x}_2, \dots, \mathbf{x}_N\}$ be a set of points to be clustered. To apply spectral clustering, we first compute an affinity matrix \mathbf{S} between every pair of data points. The affinity matrix is used to construct an undirected weighted graph $\mathcal{G} = (V, E)$, where V is the set of vertices (one for each data point) and E is the set of edges between pairs of vertices. The weight of each edge is given by the affinity between the corresponding pair of data points. The Laplacian matrix of the graph is defined as $\mathbf{L} = \mathbf{D} - \mathbf{S}$, where \mathbf{D} is a diagonal matrix whose diagonal elements correspond to $\mathbf{D}_{ii} = \sum_j \mathbf{S}_{ij}$. The goal of spectral clustering is to create a set of partitions on the graph \mathcal{G} in such a way that minimizes the graph cut while maintaining a balanced size of the cluster partitions [29].

The spectral clustering solution can be found by solving the following optimization problem [29]:

$$\arg \min_r r^T \mathbf{L} r \text{ s.t. } r^T \mathbf{D} r = \sum_i \mathbf{D}_{ii}, \mathbf{1}^T \mathbf{D} r = \mathbf{0} \quad (2)$$

where $\mathbf{1}$ and $\mathbf{0}$ are vectors whose elements are all 1s and 0s, respectively. The solution for r is obtained by solving the following generalized eigenvalue problem: $\mathbf{L} r = \lambda \mathbf{D} r$. To obtain k clusters, we first extract the top k generalized eigenvectors and apply a standard clustering algorithm such as k-means to the data matrix generated from the eigenvectors.

3.3 Constrained Spectral Clustering

Current methods for incorporating constraints into spectral clustering algorithms can be divided into two categories. The first category encompasses methods that directly alter the graph Laplacian matrix, e.g., by applying a weighted sum between the feature similarity matrix \mathbf{S} and the constraint matrix \mathbf{C} given in Equation (1):

$$\text{Weighted sum: } \mathbf{S}^{\text{total}}(\delta) = (1 - \delta)\mathbf{S} + \delta\mathbf{C}, \quad (3)$$

$\delta \in [0, 1]$ is a parameter that controls the trade-off between maximizing cluster homogeneity and preserving the constraints of the data. When δ approaches zero, the clustering solution is more biased towards maximizing the feature similarity whereas when δ approaches one, it is more biased towards preserving the constraints.

Let \mathbf{D} and $\mathbf{D}^{(c)}$ be the diagonal matrices constructed from the feature similarity matrix (\mathbf{S}) and constraint matrix (\mathbf{C}) in the following way:

$$\mathbf{D}_{ii} = \sum_j \mathbf{S}_{ij}, \quad \mathbf{D}_{ii}^{(c)} = \sum_j \mathbf{C}_{ij}.$$

Using Equation (3), it can be shown that the modified graph Laplacian is given by a convex combination of the graph Laplacian for the feature similarity matrix and the graph Laplacian for the constraint matrix, i.e.,

$$\begin{aligned} \mathbf{L}^{\text{total}} &= \mathbf{D}^{\text{total}} - \mathbf{S}^{\text{total}} \\ &= (1 - \delta)(\mathbf{D} - \mathbf{S}) + \delta(\mathbf{D}_c - \mathbf{C}) \end{aligned} \quad (4)$$

The weighted sum approach described above is a special case of the spectral constraint modeling (SCM) algorithm proposed by Shi et al. [43]. The altered graph Laplacian can be substituted into Equation (2), which in turn, allows us to apply existing spectral clustering algorithm to identify the regions.

$$\begin{aligned} \text{SCM: } \quad & \arg \min_{r \in \mathbb{R}^N} r^T \mathbf{L}^{\text{total}} r \\ \text{s.t. } & r^T \mathbf{D}^{\text{total}} r = \sum_i \mathbf{D}_{ii}^{\text{total}}, \quad \mathbf{1}^T \mathbf{D}^{\text{total}} r = \mathbf{0}. \end{aligned} \quad (5)$$

The second category of approaches for incorporating domain constraints is to alter the feasible solution set of the spectral clustering algorithm. For example, Wang and Davidson [51] proposed the CSP algorithm, which optimizes the following objective function.

$$\begin{aligned} \text{CSP: } \quad & \arg \min_{r \in \mathbb{R}^N} r^T \bar{\mathbf{L}} r \\ \text{s.t. } & r^T \bar{\mathbf{C}} r \geq \alpha, \quad r^T r = \text{vol}(\mathcal{G}), \quad r \neq \mathbf{D}^{1/2} \mathbf{1}, \end{aligned} \quad (6)$$

where $\bar{\mathbf{L}} = \mathbf{D}^{-1/2} \mathbf{L} \mathbf{D}^{-1/2}$ and $\bar{\mathbf{C}} = \mathbf{D}_c^{-1/2} \mathbf{C} \mathbf{D}_c^{-1/2}$ are the normalized graph Laplacian and normalized constraint matrix, respectively. The threshold α gives a

lower bound on the amount of constraints in \mathbf{C} that must be satisfied by the clustering solution. Instead of setting the parameter for α , Wang and Davidson [51] requires users to specify a related parameter β , which was shown to be a lower bound for α .

4 Spatially Constrained Spectral Clustering

In this section, we describe the various ways to represent spatial contiguity constraints and to incorporate them into the spectral clustering framework.

4.1 Kernel Representation of Spatial Contiguity Constraints

For constrained spectral clustering, we can define a corresponding constraint graph $\mathcal{G}_C = (V, E_C)$, where V is the set of data points and E_C is the set of edges whose weights are defined as follows:

$$E_{ij} = \begin{cases} 1, & (v_i, v_j) \text{ is a ML edge;} \\ -1, & (v_i, v_j) \text{ is a CL edge;} \\ 0, & \text{otherwise.} \end{cases} \quad (7)$$

For region delineation, the vertices of the constraint graph correspond to the set of spatial units to be clustered, while the ML edges correspond to pairs of spatial units that are adjacent to each other. It is also possible to define a CL edge between every pair of spatial units that are either located too far away from each other or are obstructed by certain barriers (e.g., large bodies of water) that make them unreasonable for assignment to the same region. However, since the number of CL edges tends to grow almost quadratically with increasing number of points, this severely affects the runtime of spectral clustering algorithm. Furthermore, the ML edges are often sufficient to provide guidance on how to form spatially contiguous regions. For these reasons, we consider constraint graphs that have ML edges only in this paper. Let \mathbf{C} denote the adjacency matrix representation of the edge set E_C .

A constrained spectral clustering algorithm is designed to produce solutions that are consistent with the constraints imposed by \mathcal{G}_C . Unfortunately, for region delineation, it may not be sufficient to use the adjacency information between neighboring spatial units to control the trade-off between spatial contiguity and landscape homogeneity of the regions. To improve its flexibility, we introduce a *spatially constrained kernel matrix*, \mathbf{S}_c . The simplest form of the kernel would be a linear kernel, which is defined as follows:

$$\text{Linear Kernel: } \quad \mathbf{S}_c^{\text{linear}} = \mathbf{C} \quad (8)$$

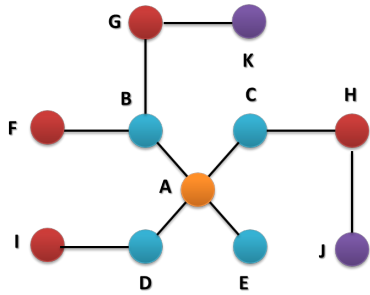


Fig. 1: An illustration of spatial contiguity constraint

More generally, we can define an exponential kernel [24] on the adjacency matrix \mathbf{C} as follows.

Exponential Kernel:

$$\mathbf{S}_c^{\text{exp}} = e^{\mathbf{C}} = \mathbf{I} + \mathbf{C} + \frac{1}{2!}\mathbf{C}^2 + \frac{1}{3!}\mathbf{C}^3 + \dots = \sum_{k=0}^{\infty} \frac{\mathbf{C}^k}{k!} \quad (9)$$

where \mathbf{I} is the identity matrix. Since we consider only ML constraints, the k -th power of the adjacency matrix \mathbf{C} represents the number of ML paths of length k that exist between every pair of vertices. An ML path between vertices (v_i, v_j) refers to a sequence of ML edges e_1, e_2, \dots, e_m such that the initial vertex of e_1 is v_i and the terminal vertex of e_m is v_j . It can be shown that $\mathbf{S}_c^{\text{exp}}$ is a symmetric, positive semi-definite matrix, and thus, is a valid kernel [24]. Furthermore, as the diameter of the constraint graph is finite, we also consider a truncated version of the exponential kernel:

$$\text{Truncated Exponential : } \mathbf{S}_c^{\text{trunc}}(\delta) \equiv \sum_{k=0}^{\delta} \frac{\mathbf{C}^k}{k!} \quad (10)$$

where the parameter δ controls the ML neighborhood size of a vertex. The ML neighborhood specifies the set of vertices that should be in the same region as the vertex under consideration. As an example, consider the graph shown in Figure 1. When $\delta = 1$, the ML neighborhood for vertex A corresponds to its immediate neighbors, B, C, D and E. When $\delta = 2$, the ML neighborhood of vertex A is expanded to include vertices that are located within a path of length 2 or less from A, i.e., B, C, D, E, F, G, H and I. When $\delta = 3$, the ML neighborhood for vertex A includes all of the vertices in the graph. Note that each term in the summation given in Equation (9) is normalized by the path length; therefore, a vertex that is located further away from a given vertex has less influence as compared to a nearer vertex.

Finally, the truncated exponential kernel matrix can be binarized so that it can be interpreted as an adjacency matrix for an expanded constraint graph, whose

ML neighborhood size is given by the parameter δ .

Binarized Truncated Exponential Kernel :

$$\mathbf{S}_c^{\text{bin}}(\delta) \equiv \mathbf{I} \left[\sum_{k=0}^{\delta} \mathbf{C}^k > 0 \right] \quad (11)$$

where $\mathbf{I}[\cdot]$ is an indicator function whose value is equal to 1 if its argument is true and 0 otherwise. Both the truncated and binarized truncated exponential kernels allow us to vary the degree to which the original constraint graph should be satisfied. As δ increases, the constraint satisfaction becomes more relaxed. Ultimately, when δ is greater than or equal to the diameter of the graph, $\mathbf{S}_c^{\text{bin}}$ reduces to a matrix of all 1s, which is equivalent to ignoring the spatial contiguity constraints.

4.2 Hadamard Product Graph Laplacian

We now describe our approach for incorporating the spatially constrained kernel matrix \mathbf{S}_c into the spectral clustering formulation. Instead of using the weighted sum approach given in Equation (3), we consider a Hadamard product approach to combine \mathbf{S}_c with the feature similarity matrix \mathbf{S} :

$$\text{Hadamard Product: } \mathbf{S}^{\text{total}}(\delta) = \mathbf{S} \circ \mathbf{S}_c(\delta), \quad (12)$$

where $\mathbf{S}_c(\delta)$ corresponds to either the truncated exponential kernel (Equation (10)) or the binarized truncated exponential kernel (Equation (11)).

There are several advantages to using a Hadamard product approach to combine the matrices. First, unlike the weighted sum approach, it discourages spatial units that are located far away from each other from being assigned to the same cluster even though their feature similarity is high. Second, it produces a sparser kernel matrix, which is advantageous for large-scale graph analysis. Finally, it gives more flexibility to the users to specify the level of constraints that must be preserved by tuning the parameter δ , which controls the ML neighborhood size of the constraint graph.

Let $\mathbf{D}_{ii}^{\text{total}} = \sum_j [\mathbf{S} \circ \mathbf{S}_c(\delta)]_{ij}$ be elements of a diagonal matrix computed from $\mathbf{S}^{\text{total}}$. The Hadamard product graph Laplacian is given by $\mathbf{L}^{\text{total}} = \mathbf{D}^{\text{total}} - \mathbf{S} \circ \mathbf{S}_c(\delta)$. The modified graph Laplacian can be substituted into Equation (2) and solved using the generalized eigenvalue approach to identify the regions.

4.3 Partitional Spatially-Constrained Spectral Clustering Algorithm

Algorithm 1 presents a high-level overview of our partitional clustering approach. First, a feature similarity

Algorithm 1 Partitional Spatially-Constrained Spectral Clustering

Input:

$\mathcal{D} = \{(\mathbf{x}_1, \mathbf{s}_1), (\mathbf{x}_2, \mathbf{s}_2), \dots, (\mathbf{x}_N, \mathbf{s}_N)\}$
 $\mathbf{C} \in R^{N \times N}$: spatial constraint matrix.
 k : number of clusters.
 δ : neighborhood size.

Output:

$\mathcal{R} = \{R_1, R_2, \dots, R_k\}$ (set of regions).

1. Create similarity matrix \mathbf{S} from $\{\mathbf{x}_1, \mathbf{x}_2, \dots, \mathbf{x}_N\}$.
 2. Compute the spatially constrained kernel matrix, $\mathbf{S}_c(\delta)$.
 3. Compute the combined kernel $\mathbf{S}^{\text{total}}$ based on \mathbf{S} and \mathbf{S}_c .
 4. Compute $\mathbf{D}^{\text{total}}$ and $\mathbf{L}^{\text{total}}$.
 5. Solve the generalized eigenvalue problem $\mathbf{L}^{\text{total}} \mathbf{r} = \lambda \mathbf{D}^{\text{total}} \mathbf{r}$. Create matrix $\mathbf{X}_r = [r_1 r_2 \dots r_k]$ from the top- k eigenvectors.
 6. $\mathcal{R} \leftarrow \text{k-means}(\mathbf{X}_r, k)$
-

matrix is created by applying the Gaussian radial basis function kernel, $k(\mathbf{x}_i, \mathbf{x}_j) = \exp(-\frac{\|\mathbf{x}_i - \mathbf{x}_j\|^2}{2\sigma^2})$ to the feature set of the spatial units. The spatially constrained kernel matrix \mathbf{S}_c is then computed from the constraint matrix \mathbf{C} , where $\mathbf{C}_{ij} = 1$ if $(\mathbf{s}_i, \mathbf{s}_j)$ is a ML edge and 0 otherwise. Note that if the truncated exponential kernel is used to represent the spatially constrained kernel matrix, we termed the approach as a spatially-constrained spectral clustering (SSC) algorithm. However, if the binarized truncated exponential kernel is used, the approach is known as a binarized spatially-constrained spectral clustering (BSSC).

Once the combined graph Laplacian, $\mathbf{L}^{\text{total}}$ is found, we extracted the first k eigenvectors as the low rank approximation of the combined kernel matrices. We then applied k-means clustering to partition the data into its respective regions. Note that the partitional clustering framework shown in Algorithm 1 is also applicable to the SCM and CSP algorithms, by setting their corresponding graph Laplacian, $\mathbf{L}^{\text{total}}$ and diagonal matrix, $\mathbf{D}^{\text{total}}$. The computational complexity of the spatially constrained spectral clustering is equivalent to the standard spectral clustering algorithm, which is $O(N^3)$.

4.4 Hierarchical Spatially-Constrained Spectral Clustering Algorithm

The formulation described in the previous section can be extended to hierarchical clustering by using a recursive bisection approach. Specifically, the algorithm will iteratively identify the least homogeneous region to be split into two smaller subregions until every subregion contains only a single spatial unit.

The pseudocode of the proposed algorithm is shown in Algorithm 2. First, the feature similarity matrix \mathbf{S}

Algorithm 2 Hierarchical Spatially-Constrained Spectral Clustering (HSSC)

Input:

$\mathcal{D} = \{(\mathbf{x}_1, \mathbf{s}_1), (\mathbf{x}_2, \mathbf{s}_2), \dots, (\mathbf{x}_N, \mathbf{s}_N)\}$
 $\mathbf{C} \in R^{N \times N}$: spatial constraint matrix.
 δ : neighborhood size.

Output:

$\mathcal{R} = \{R_1, R_2, \dots, R_k\}$ (set of regions).

1. Create similarity matrix \mathbf{S} from $\{\mathbf{x}_1, \mathbf{x}_2, \dots, \mathbf{x}_N\}$.
 2. Compute the spatially constrained kernel matrix, $\mathbf{S}_c(\delta)$.
 3. Compute the combined kernel $\mathbf{S}^{\text{total}}$ based on \mathbf{S} and \mathbf{S}_c .
 4. Compute $\mathbf{D}^{\text{total}}$ and $\mathbf{L}^{\text{total}}$.
 5. Initialize R_1 as the cluster containing all N spatial units.
 6. **for** $k = 2$ to N **do**
 - 6a. $C^* = \text{choose}(R_{k-1})$
 - 6b. $R_k \leftarrow R_{k-1} - C^*$
 - 6c. $(C_1, C_2) \leftarrow \text{SSC}(\mathcal{D}_{C^*}, 2)$
 - 6d. $R_k \leftarrow R_{k-1} \cup \{C_1, C_2\}$.
-

is computed using the Gaussian RBF kernel function. Next, the spatial constraint matrix $\mathbf{S}_c(\delta)$ is created using Equation 11. The algorithm will then compute the combined kernel $\mathbf{S}^{\text{total}}$ and its corresponding graph Laplacian matrix $\mathbf{L}^{\text{total}}$, similar to the approach described in Section 3.3. The algorithm initially assigns all the data points to a single cluster. It then recursively partitions the data until k clusters are obtained, as shown in lines 6a-6d in Algorithm 2. Let R_{k-1} be the set of clusters found after $k - 1$ iterations. On line 6a, the algorithm chooses the cluster $C^k \in R_{k-1}$ with the worst sum of square within errors (SSW) to be split into two smaller clusters, C_1 and C_2 (line 6c). One advantage of using our top-down recursive partitioning approach is that neither the feature similarity nor the spatial constraint matrix have to be updated at each iteration unlike the bottom-up hierarchical clustering, which requires us to re-compute the modified feature similarity and constraint matrices each time a pair of clusters is merged.

5 Application to Region Delineation

To evaluate the effectiveness of constrained spectral clustering for region delineation, we conducted a case study on a large-scale terrestrial ecology data set. The results of the case study are presented in this section.

5.1 Data set

The constrained spectral clustering methods were assessed using geospatial data from the LAGOS_{GEO} [46,

47] database. The database contains landscape characterization features measured at multiple spatial scales with a spatial extent that covers a land area spanning 17 U.S. states. The land area was divided into smaller hydrologic units (HUs), identified by their 12-Digit Hydrologic Unit Code [41]. Our goal was to develop a regionalization system for the landscape by aggregating the 20,257 HUs into coarser regions. We selected 28 terrestrial landscape variables and performed experiments on three study areas—Michigan, Iowa, and Minnesota. When the values for a landscape variable was always zero, we removed that variable before applying the clustering methods. The number of HUs to be clustered in each study region, as well as number of landscape variables for each, are summarized in Table 1.

The data set was further preprocessed before applying the constrained clustering algorithms. First, each variable was standardized to have a mean value of zero and variance of one. Since some of the landscape variables were highly correlated, we applied principal component analysis to reduce the number of features, keeping only the principal components that collectively explained at least 85% of the total variance. The principal component scores were then used to calculate a feature similarity matrix for all pairs of HUs in each study area. The ML edges for the constraint graph were determined based on whether the polygons for two HUs were adjacent to each other.

5.2 Baseline Methods

For partitional-based constrained clustering, we compared our algorithms, SSC and BSSC, against three competing baseline methods. The first baseline, called SCM [43], uses a weighted sum approach (Equation (3)) to combine the feature similarity matrix \mathbf{S} with the adjacency matrix \mathbf{C} of the constraint graph. The algorithm has a parameter $\delta \in [0, 1]$ that controls whether the clustering should favor homogeneity or spatial contiguity of the regions. When δ approaches 0, the algorithm is biased towards maximizing the similarity of features in the regions whereas when δ approaches 1, it is biased towards producing more contiguous regions.

The second baseline method, called CSP [51], uses the spatial constraints to restrict the feasible set of the clustering solution (Equation (6)). As noted in Section 3.3, the algorithm has a parameter β that gives a lower bound on the proportion of constraints that must be satisfied by the clustering solution. Furthermore, $\beta < \lambda_{\max} \text{vol}(\mathcal{G})$ to ensure the existence of a feasible solution [51]. Instead of using β , we define an equivalent tuning parameter $\delta = \beta / [\lambda_{\max} \text{vol}(\mathcal{G})]$ so that its upper bound,

which is equal to 1, is consistent with the upper bound for other algorithms evaluated in this study.

The third baseline is a spatially constrained clustering method proposed recently in the ecology literature by Miele et al. [32]. It uses a stochastic model to represent nodes and links in a spatial ecological network. The cluster membership of each node is assumed to follow a multinomial distribution. Spatial constraints are introduced as a regularization penalty in the maximum likelihood estimation of the model parameters. The algorithm is implemented as part of the Geoclust R package. We denote the model-based method as MB in the remainder of this paper.

For hierarchical clustering, we compare our proposed HSSC algorithm against the space-constrained clustering method described in [26]. The method is similar to traditional agglomerative hierarchical clustering, except it applies a Hadamard product between the feature similarity matrix \mathbf{S} with the spatial constraint matrix \mathbf{S}_c to generate a combined similarity matrix $\mathbf{S}^{\text{total}}$. This is identical to the approach used in HSSC. The agglomerative clustering algorithm initially assigns each spatial unit to be in its own cluster (region). It then merges the two clusters with the highest similarity value in $\mathbf{S}^{\text{total}}$. Both the feature similarity matrix \mathbf{S} and the spatial constraint matrix \mathbf{S}_c are then updated accordingly. The update for \mathbf{S} depends on how the similarity between two clusters is computed. Among the popular approaches that have been used to update \mathbf{S} include single link [44], complete link [48], group average (UPGMA) [45], and the Ward’s method [52]. The adjacency matrix \mathbf{C} is updated based on whether there is a path from any point in one cluster to any point in the other cluster and the constrained similarity matrix \mathbf{S}_c is updated based on Equation 10 with a predefined δ .

We implemented SCM, SSC, BSSC, HSSC and the spatially constrained agglomerative hierarchical clustering (single link, complete link, UPGMA, Ward’s method) in Matlab. For CSP and MB, we downloaded their software from the links provided by the authors¹.

5.3 Evaluation Metrics

We evaluated the performance of the algorithms based on three criteria: homogeneity, spatial contiguity, and region size. To determine whether the regions were ecologically homogeneous, we computed their within-cluster

¹ CSP was obtained from <https://github.com/gnaixgnaw/CSP> whereas MB was downloaded from <http://1bbe.univ-lyon1.fr/Download-5012.html?lang=fr>.

Table 1: Summary statistics of the data set

Study Area	# HUs	# landscape variables	# PCA components	Diameter of constraint graph
Michigan	1,796	17	10	41
Iowa	1,605	19	12	43
Minnesota	2,306	19	11	57

sum-of-square error (SSW) [49]:

$$SSW = \sum_{i=1}^k \sum_{x \in C_i} dist(\mu_i, x)^2 \quad (13)$$

where μ_i is the centroid of the cluster C_i . The lower SSW is, the more homogeneous are the spatial units within the regions.

The second criteria assesses the spatial contiguity of the resulting regions. We consider two metrics for this evaluation. The first metric computes the percentage of ML constraints preserved within the regions:

$$PctML = \frac{\# \text{ ML edges within discovered regions}}{\text{Total \# of ML edges}} \quad (14)$$

The second metric corresponds to a relative contiguity metric proposed in the ecology literature by Wu and Murray [55]. The metric takes into consideration both the within patch contiguity (ϕ) and between patch contiguity (ν):

$$c = \frac{\phi + \nu}{\Omega} \quad (15)$$

where

$$\phi = \sum_{i=1}^k \left(\frac{N_i(N_i - 1)}{2} \right), \quad \nu = \frac{1}{2} \sum_{i=1}^k \sum_{j=1, j \neq i}^k \left(\frac{N_i N_j}{l_{ij}^\gamma} \right)$$

$$\Omega = \frac{(\sum_{i=1}^k N_i)(\sum_{i=1}^k N_i - 1)}{2}$$

In the preceding formula, k is the number of regions and N_i is the number of spatial units assigned to the i -th region. l_{ij} denote the minimum spanning tree path length between regions i and j while γ is a distance decay parameter. Since the metric is normalized by the total number of possible edges in a complete graph (Ω), it ranges between 0 and 1.

Although spatial contiguity is a desirable criterion, it may lead to highly imbalanced regions [33]. For example, an algorithm that creates one very large region along with many smaller but contiguous regions will likely have a high contiguity value. Previous studies [13, 5] have shown the importance of maintaining a more balanced cluster sizes to ensure good clustering performance. Thus, given a set of k clusters with their corresponding cluster sizes, n_1, n_2, \dots, n_k , we define a metric,

$Cbalance$, based on the normalized geometric mean of the cluster sizes:

$$Cbalance = \frac{k}{N} \left[n_1 \times n_2 \times \dots \times n_k \right]^{\frac{1}{k}}, \quad (16)$$

where N is the total number of data points and k is the number of clusters. The metric ranges from 0 to 1 and the larger the value, the more balanced are the cluster sizes.

5.4 Results and Discussion

This section presents the results of applying various clustering algorithms to the terrestrial ecology data.

5.4.1 Tradeoff between Homogeneity and Spatial Contiguity

We first analyze the trade-off between landscape homogeneity and spatial contiguity of the regions by comparing the results for four partitional constrained spectral clustering algorithms: SCM, CSP, SSC, and BSSC. The number of clusters was set to 10. As each algorithm has a parameter δ that determines whether the clustering should be more biased towards increasing the within-cluster similarity or preserving the ML constraints, we varied the parameter and assessed their performance using the metrics described in Section 5.3. The δ parameter for SSC and BSSC has been re-scaled to a range between 0 and 1 by dividing the ML neighborhood size with the diameter of the constraint graph.

The results are shown in Figure 2. Observe that the contiguity score (c and PctML) for SCM increases rapidly as δ becomes closer to 1. This is because increasing δ would bias the algorithms towards preserving the spatial constraints. A similar increasing trend was also observed for CSP, especially in Iowa and Michigan, though the increase is not as sharp as SCM. In contrast, the contiguity scores would decrease for BSSC as δ increases because it creates more new ML edges involving spatial units that are not adjacent to each other. For SSC, the contiguity scores do not appear to change by much as δ increases. This is because the weight $1/k!$ associated with each path of length k decreases rapidly

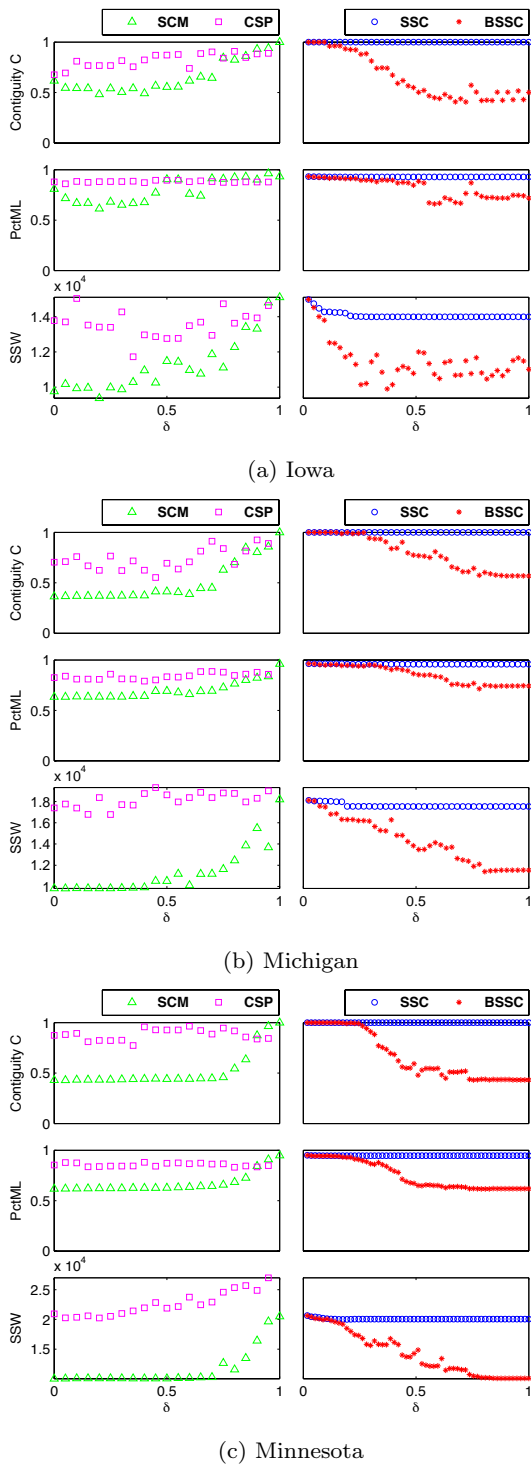


Fig. 2: Comparison between various constrained spectral clustering algorithms in terms of their landscape homogeneity (SSW) and spatial contiguity (PctML and c). The horizontal axis in the plots corresponds to the parameter value δ .

to zero as k increases. As a consequence, the ML neigh-

borhood size for SSC grows until it reaches a maximum size by which increasing δ will not significantly alter the constraint graph. Thus, SSC is less sensitive to parameter tuning compared to BSSC. Figure 2 also shows there is generally an increasing trend in SSW for SCM and CSP as δ increases. For SSC, the SSW values do not appear to change significantly with increasing δ whereas for BSSC, the SSW curve decreases monotonically as the neighborhood size increases.

The results of this study showed that the trade-off between landscape homogeneity and spatial contiguity varies among the constrained spectral clustering algorithms. For CSP and SSC, the parameters provided by the algorithms do not allow us to achieve the full range of SSW and contiguity scores. Although these algorithms can produce regions with high contiguity scores, their SSW values were also very high. In contrast, with careful parameter tuning, SCM and BSSC can produce regions with significantly lower SSW compared to CSP and SSC. Observe that the slopes of the curves are steeper near $\delta = 1$ for SCM, which suggests that decreasing δ below 1 would lead to a dramatic reduction in the contiguity score and SSW of the regions. This makes it harder for SCM to produce regions that are both spatially contiguous and homogeneous. In contrast, the curves for the contiguity scores of BSSC are flatter near $\delta = 0$. This enables the BSSC algorithm to produce regions with homogeneous landscape features yet are still spatially contiguous.

5.4.2 Performance Comparison for Partitional-based Constrained Clustering

In this experiment, we set the number of clusters to 10 and selected the δ parameter that gives the highest contiguity score for each constrained spectral clustering method. If there are more than one parameter values that achieve the highest contiguity score, we chose the one with lowest SSW. For MB, since the Geoclust R package did not support parameter tuning by users, we applied the algorithm using its default setting.

Table 2 summarizes the results of our analysis. SCM, SSC, and BSSC can be tuned to produce regions that are fully contiguous ($c = 1$). The SSW for BSSC and SSC are consistently better than SCM. These results clearly showed the advantage of using a Hadamard product approach instead of a weighted sum approach to integrate spatial constraints into the feature similarity matrix. The limitation of using a weighted sum approach can be explained as follows. Since the highest contiguity score is achieved by setting $\delta = 1$, the clustering solution of SCM is equivalent to applying spectral clustering on the constraint graph only, without

Table 2: Performance comparison among various partitional spatially-constrained clustering algorithms with the number of clusters set to 10.

States	Method	PctML	c	SSW	Cbalance
IA	SCM	93.26%	1.00	15104	0.95
	CSP	87.37%	0.91	13628	0.19
	MB	89.95%	0.69	18997	0.34
	SSC	92.83%	1.00	13993	0.95
	BSSC	92.40%	1.00	14001	0.94
MI	SCM	96.08%	1.00	18200	0.85
	CSP	87.81%	0.92	18307	0.44
	MB	88.76%	0.65	16091	0.91
	SSC	95.69%	1.00	17534	0.92
	BSSC	94.92%	1.00	17485	0.93
MN	SCM	94.78%	1.00	20506	0.91
	CSP	86.62%	0.96	23755	0.69
	MB	88.96%	0.64	20400	0.67
	SSC	94.57%	1.00	19998	0.93
	BSSC	94.12%	1.00	19594	0.91

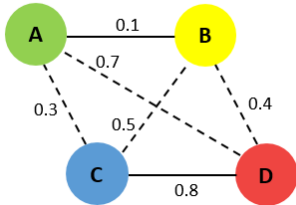


Fig. 3: A toy example illustrating the advantage of using Hadamard product for combining constraints with feature similarity. Each labeled node is a data point, with a solid line representing a must-link constraint between two points and a dashed line representing the absence of such constraint. The weight of each edge denotes the feature similarity between two data points.

considering the feature similarity. If we reduce the parameter value to, say $\delta = 0.95$, its contiguity score decreases sharply (see Figure 2) while its SSW value is still worse than BSSC. The weighted sum approach has poor SSW because it significantly alters the feature similarity matrix.

To illustrate the limitation of using the weighted sum approach, consider the toy example shown in Figure 3. Assume there are 4 data points: A, B, C and D, that need to be clustered. A sample of their pairwise similarity values is shown in Table 3.

Although the A-B pair has a significantly lower similarity value than C-D, the weighted sum approach inflates the similarity significantly (assuming $\delta = 0.95$) which makes it overall similarity to be comparable to C-D. In contrast, the Hadamard product approach simply zeros out the similarity of pairs that do not have ML

Table 3

Pairs	Feature Similarity	ML Constraint	Weighted Sum	Hadamard Product
A-B	0.1	1	0.955	0.1
B-C	0.5	0	0.025	0
C-D	0.8	1	0.990	0.8

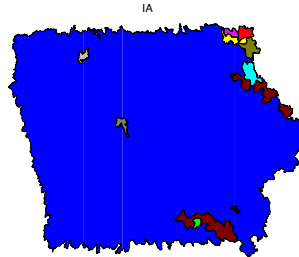


Fig. 4: Regions for Iowa created by the SCM algorithm using the weighted sum approach (with $\delta = 0.95$).

edges, and thus, will not artificially inflate the similarities of pairs with ML edges.

Furthermore, since the feature similarity is computed using Gaussian radial basis function (see Section 4.3), the resulting matrix \mathbf{S} for the weighted sum approach is still dense after incorporating the spatial constraints. Unless $\delta = 1$, the weighted sum approach will not prevent spatial units that are located far from each other from being placed into the same region. For example, consider the regions found by the weighted sum approach for Iowa, as shown in Figure 4. Although the regions appear to be spatially contiguous, they are not compact and have varying sizes. In fact, most of the spatial units were assigned to the same region when $\delta = 0.95$. Even at the lower δ threshold, its SSW (14805) is still the worse than the SSW for our framework and CSP.

The contiguity scores for MB are worse than other constrained clustering methods. Nevertheless, it preserves at least 88% of the ML edges within the regions. Except for Michigan, its SSW values are also worse than other methods. In contrast, CSP has the lowest contiguity score among all the constrained spectral clustering methods. Except for Iowa, its SSW values are also among the worst. The limitation of CSP [51] is a consequence of the parameter used to control its spatial contiguity. As shown in Equation (6), the level of spatial constraints satisfied by the clustering solution depends on the parameter α . However, instead of directly tuning α , the authors suggested to vary another parameter, β , which was shown to be an upper bound of α . The results of our case study showed that increasing the value of β does not necessarily imply an increase in α . To illustrate this point, we randomly generated a constraint

graph that has nine vertices with a randomly generated feature similarity matrix. Assuming the number of clusters is equal to 2, we ran the CSP algorithm with different parameter settings and plotted their values of α and β in Figure 6. Although this figure shows that the value of β (blue diamond) is a lower bound of α (red circle), the bound is so loose that it can not guarantee that increasing β will increase α . In fact, the figure on the right shows that α is not a monotonically increasing function of β . This is why controlling its parameter value will not always guarantee that the regions will be contiguous even when $\delta = 1$ (unlike SCM and the Hadamard product approaches).

In terms of the Cbalance measure, our results suggest that SCM, SSC, and BSSC achieve the highest cluster balance for all three states. This can be verified by examining the regions generated by all the competing algorithms for the the state of Michigan, as shown in Figure 5². As can be seen from the figure, the regions produced by SCM, SSC, and BSSC are more compact and uniform in size compared to CSP and MB. However, the SSW for SCM is worse than the SSW for our proposed SSC and BSSC algorithms. This is not surprising as SCM cannot produce contiguous clusters unless δ is very close to 1. If δ is lowered slightly to 0.95, the regions changed significantly, as shown in Figure 4. By setting δ close to 1, SCM will focus only on preserving the spatial constraints, and thus, has worse cluster homogeneity compared to our algorithms. Thus, our results clearly show the benefits of applying BSSC to develop homogeneous and spatially contiguous regions compared to other baseline algorithms. These results hold true even when the number of regions is varied. A comparison of the results for different number of clusters can be found in our earlier work [56].

5.4.3 Performance Comparison for Hierarchical-based Constrained Clustering

In this section, we compared our proposed HSSC algorithm against the spatially-constrained agglomerative clustering methods for constructing nested regions. Note that all of the algorithms apply a Hadamard product to combine the constrained matrix \mathbf{S}_c (for a given δ) with the feature similarity matrix \mathbf{S} to generate the combined matrix $\mathbf{S}^{\text{total}}$ before applying hierarchical clustering. For the spatially-constrained agglomerative hierarchical clustering methods, the regions are iteratively merged starting from the initial $\mathbf{S}^{\text{total}}$.

For a fair comparison, we set $\delta = 1$ for all the methods. The results for $k = 10$ are summarized in Table

4. In terms of region contiguity, observe that all the methods can achieve $c = 1$. However, the spatially constrained complete link and UPGMA algorithms produce the highest PctML values while the Ward’s method produces the lowest value. The PctML for our proposed HSSC algorithm is still relatively high and comparable to its non-hierarchical counterparts, SSC and BSSC (see Table 2). Despite their high spatial contiguity, both the spatially-constrained complete link and UPGMA methods have the worst SSW compared to other methods. Worst still, their Cbalance values are close to 0, suggesting that the sizes of their regions are highly imbalanced. This can be seen from the maps shown in Figure 7, where there is a large region covering the majority of the landscape in each state. In contrast, our HSSC algorithm has the highest Cbalance, consistently producing regions that are compact and approximately similar in sizes.

The spatially-constrained single link method has comparable PctML but slightly lower SSW compared to HSSC. It also suffers from the same imbalance region problem as the complete link and UPGMA methods. Meanwhile, the spatially-constrained Ward’s method achieves the lowest SSW among all the competing methods, which is not surprising since the algorithm is designed to minimize the SSW in each iteration of the algorithm. However, this comes at the expense of its poor PctML values, which is the worst among all the competing methods. In addition, the Ward’s method is known to suffer from the cluster inversion problem [33], in which its objective function is not monotonically non-decreasing as the number of clusters increases. In short, our HSSC algorithm outperforms the complete link, UPGMA, and Ward’s methods in 2 of the 3 evaluation criteria. Its PctML and SSW is also quite similar to single link, which suffers from the region imbalanced problem.

Figures 8a and 8b show a comparison between the regions produced by BSSC, HSSC, and the Ward’s method for the state of Michigan as we vary the number of regions from 4 to 10. We show the value of the unnormalized δ along with four metrics— c , PctML, SSW, and Cbalance—at the top of each diagram. Recall that the normalized δ is the ratio between the original δ given in Equation (7) and the diameter of the spatial constraint graph. As we increase δ from 1/41 to 4/41, the Ward’s method no longer produces regions that are contiguous unlike the BSSC and HSSC methods. The Cbalance for Ward’s method is also worse than our algorithms except when the number of clusters is small. The results for BSSC is quite comparable to HSSC, since both of them are based on the same spatially constrained spectral clustering framework. The Cbal-

² The corresponding maps of regions for other states can be found in [56].

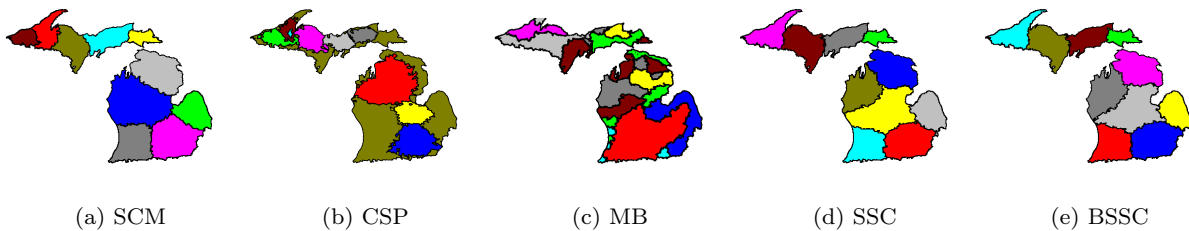


Fig. 5: Regions created by the SCM, CSP, MB, SSC and BSSC algorithms for the state of Michigan.

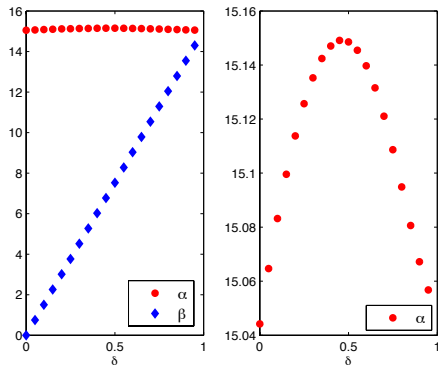


Fig. 6: The relationship between α and β parameter values for the CSP algorithm when applied to a synthetic graph data.

Table 4: Performance comparison among various hierarchical spatially-constrained clustering algorithms with $\delta = 1$ and the number of clusters set to 10.

States	Method	PctML	c	SSW	Cbalance
IA	HSSC	92.53 %	1	15080	0.92
	Single link	96.02 %	1	14191	0.04
	Complete link	98.75 %	1	18309	0.02
	UPGMA	98.45 %	1	18227	0.02
	Ward's	84.96 %	1	9281	0.48
MI	HSSC	95.41 %	1	17420	0.86
	Single link	95.31 %	1	16575	0.08
	Complete link	98.72 %	1	20083	0.03
	UPGMA	98.33 %	1	19441	0.04
	Ward's	86.28 %	1	14047	0.79
MN	HSSC	95.02 %	1	20075	0.82
	Single link	90.70 %	1	19660	0.20
	Complete link	99.17 %	1	33431	0.01
	UPGMA	98.81 %	1	28681	0.02
	Ward's	87.69 %	1	14183	0.63

ance and SSW for HSSC are slightly better than BSSC but its PctML is slightly worse. While this may seem counter-intuitive since BSSC directly optimizes the objective function for spatially-constrained spectral clustering whereas HSSC uses a greedy recursive bisection strategy, it is worth noting that the objective function does not depend solely on the feature similarities within

the regions. Instead, it takes into account the spatial constraint matrix C as well. In fact, if we compare the values of the objective functions for BSSC and HSSC at $k = 10$ for the state of Michigan, BSSC has a noticeably lower value (13458.13) compared to HSSC (14284.21).

Finally, we also compare the stability of the regions as we increase ML neighborhood size (δ). For this experiment, we show the results for the state of Michigan (in which the diameter of the constraint graph is 41) and varies the normalized δ from $1/41$ to $4/41$. We use the adjusted rand index [36] to compare the similarity between two clustering results. A high adjusted rand index would suggest that the regions found are stable, i.e., do not vary significantly with different values of δ . Table 5 shows the mean adjusted rand index (averaged over the number of clusters, which varies from 1 to 10) for HSSC, BSSC, and Ward's method. The results suggest that the proposed BSSC and HSSC methods are less sensitive to the change in δ compared to the Ward's method, which is another advantage of using our frameworks.

	BSSC	HSSC	Ward's
Mean Adjusted Rand Index	0.92	0.86	0.66

Table 5: Stability of the regions generated by different hierarchical clustering methods for the state of Michigan. The mean Adjusted Rand Index is computed for each method by comparing the similarity between the regions found with $\delta = 1/41$ to the regions found with $\delta = 4/41$.

6 Conclusions

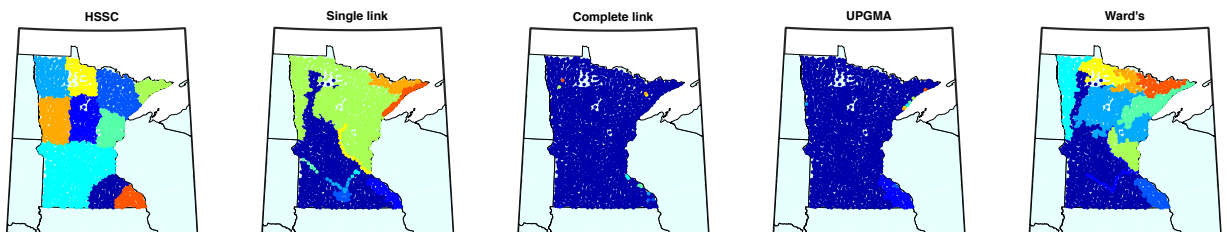
This research investigated the feasibility of applying constrained spectral clustering to the regionalization task. We compared several constrained spectral clustering methods and showed the trade-off between landscape homogeneity and spatial contiguity of their resulting regions. We presented two algorithms, SSC and



(a) Regions in IA developed by 5 hierarchical algorithm with 10 clusters



(b) Regions in MI developed by 5 hierarchical algorithm with 10 clusters



(c) Regions in MN developed by 5 hierarchical algorithm with 10 clusters

Fig. 7: Regions developed by 5 hierarchical spatially constrained clustering algorithm for 3 study regions

BSSC, that uses a Hadamard product approach to combine the similarity matrix of landscape features with spatial contiguity constraints. The results of our case study showed that the proposed BSSC algorithm is most effective in terms of producing spatially contiguous regions that are homogeneous. The extension of this algorithm to a hierarchical clustering setting also shows its advantages in producing regions that are more balanced in size compared to other hierarchical spatially-constrained algorithms. It also achieves high spatial contiguity and moderate SSW, comparable to the results of its non-hierarchical counterpart (BSSC).

7 Acknowledgements

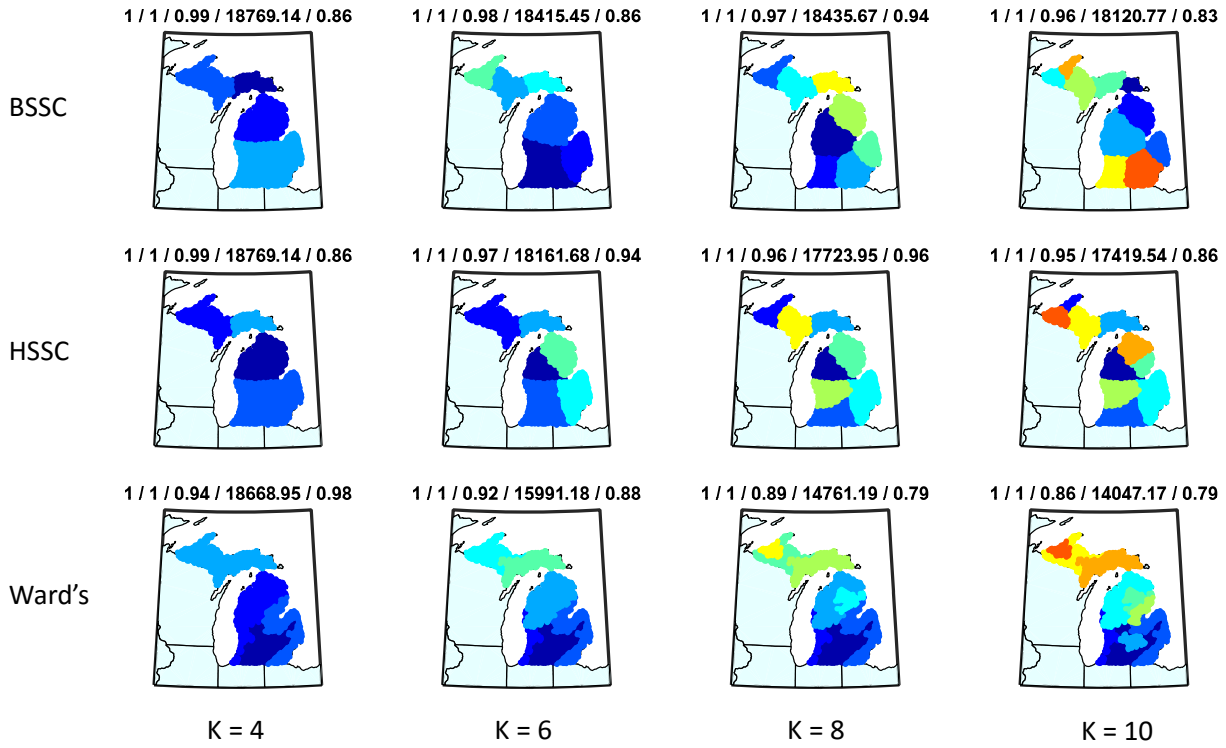
This research was funded in part by the National Science Foundation under grant #EF-1065786 and #IIS-1615612.

8 Conflict of Interest

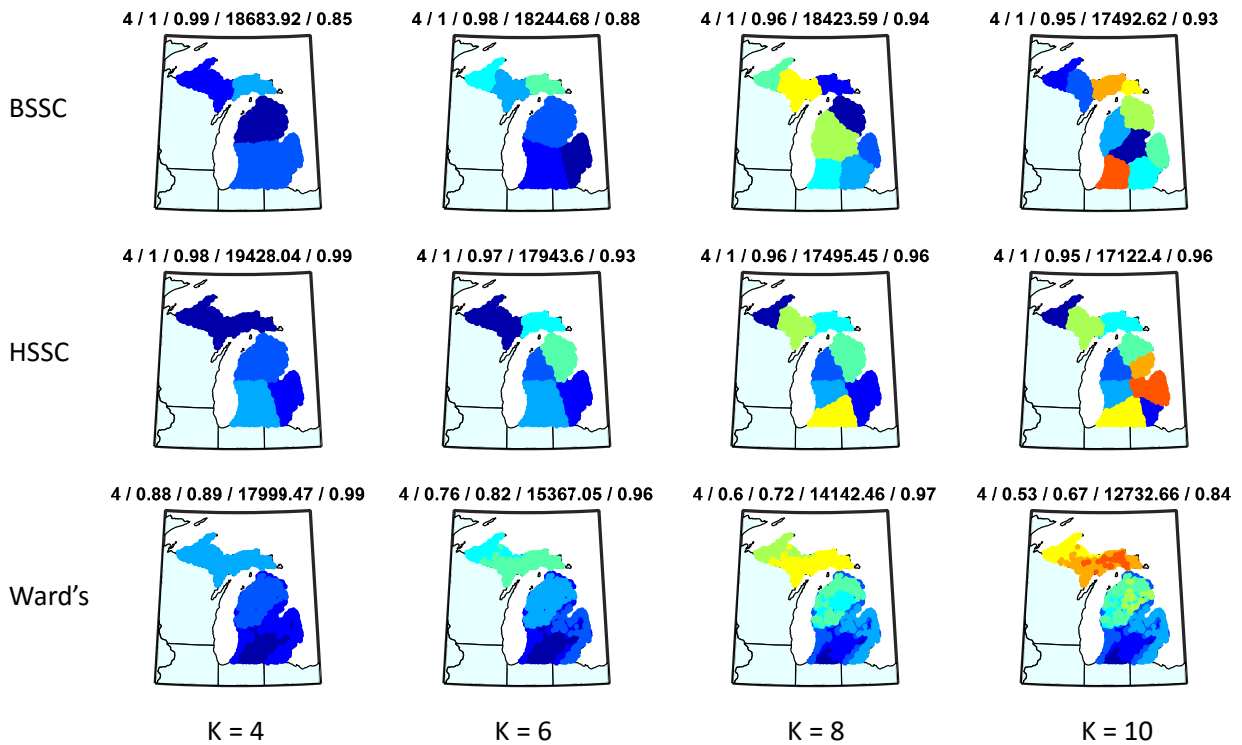
On behalf of all authors, the corresponding author states that there is no conflict of interest.

References

1. Abell, R., Thieme, M.L., Revenga, C., Bryer, M., Kottelat, M., Bogutskaya, N., Coad, B., Mandrak, N., Balderas, S.C., Bussing, W., Stiassny, M.L.J., Skelton,



(a) Results for $\delta = 1/41$



(b) Results for $\delta = 4/41$

Fig. 8: Comparison between BSSC, HSSC and Ward's method for number of cluster $K = 4, 6, 8, 10$. The five metrics evaluated are listed on top of each figure, namely: unnormalized delta, contiguity metric c , PctML preserved, SSW and cluster balance. Results for $\delta = 1/41$ are shown in (a) and results of the unnormalized $\delta = 4/41$ are shown in (b).

- P., Allen, G.R., Unmack, P., Naseka, A., Ng, R., Sindorf, N., Robertson, J., Armijo, E., Higgins, J.V., Heibel, T.J., Wikramanayake, E., Olson, D., Lpez, H.L., Reis, R.E., Lundberg, J.G., Prez, M.H.S., Petry, P.: Freshwater ecoregions of the world: A new map of biogeographic units for freshwater biodiversity conservation. *BioScience* **58** (2008)
2. Bacao, F., Lobo, V., Painho, M.: Geo-self-organizing map (geo-som) for building and exploring homogeneous regions. In: M. Egenhofer, H. Miller, C. Freksa (eds.) *GI-Science, Lecture Notes in Computer Science*, pp. 22–37. Springer, Berlin (2004)
 3. Bailey, R.G.: *Ecoregions map of north america: Explanatory note*. Miscellaneous Publication 1548 (1998)
 4. Bailey, R.G.: *Ecosystem Geography: From Ecoregions to Sites*. Springer-Verlag (2009)
 5. Banerjee, A., Ghosh, J.: Scalable clustering algorithms with balancing constraints. *Data Mining and Knowledge Discovery* **13**(3), 365–395 (2006)
 6. Basu, S., Davidson, I., Wagstaff, K.: *Constrained Clustering: Advances in Algorithms, Theory, and Applications*. Taylor and Francis (2008)
 7. Bie, T.D., Suykens, J.A.K., Moor, B.D.: Learning from general label constraints. In: *SSPR/SPR*, vol. 3138, pp. 671–679. Springer (2004)
 8. Boley, D., Kawale, J.: Constrained spectral clustering using l1 regularization. In: *SIAM Int'l Conference on Data Mining*, pp. 103–111. SIAM (2013)
 9. Cheruvelil, K., Soranno, P., Webster, K., drivers of ecosystem state: Quantifying the spatial scale. *Ecological Applications* **23**, 1603–1618 (2013)
 10. Cheruvelil, K.S., Yuan, S., Webster, K., Tan Pang-Ning, L.J.F., Collins S.M, F.C., Scott, C., Henry, E., Soranno, P., Filstrup C.T, W.T.: Creating multithemed ecological regions for macroscale ecology: Testing a flexible, repeatable, and accessible clustering method. *Ecology and evolution* **7**, 3046–3058 (2017)
 11. Craddock, R.C., James, G.A., Holtzheimer, P.E., Hu, X.P., Mayberg, H.S.: A whole brain fMRI atlas generated via spatially constrained spectral clustering. *Human brain mapping* **33**, 1914–1928 (2012)
 12. Davidson, I., Ravi, S.S.: Agglomerative hierarchical clustering with constraints: Theoretical and empirical results. In: *Lecture notes in computer science*, pp. 59–70. Springer (2005)
 13. Ding, C., He, X.: Cluster merging and splitting in hierarchical clustering algorithms. In: *Proc. IEEE Int'l Conf. Data Mining*, pp. 139–146 (2002)
 14. Duque, J.C., Ramos, R., Suriach, J.: Supervised regionalization methods: A survey. *International Regional Science Review* **30**, 195–220 (2007)
 15. George, J.A., Lamar, B.W., Wallace, C.A.: Political district determination using largescale network optimization (1997)
 16. Grygorash, O., Zhou, Y., Jorgensen, Z.: Minimum spanning tree based clustering algorithms. In: *18th IEEE International Conference on Tools with Artificial Intelligence*, pp. 73–81. Arlington, VA (2006)
 17. Han, J., Kamber, M., Tung, A.: Spatial clustering methods in data mining: A survey. In: *Geographic data mining and knowledge discovery*, pp. 188–217. Taylor and Francis (2001)
 18. Hargrove, W., Hoffman, F.: Potential of multivariate quantitative methods for delineation and visualization of ecoregions. *Environmental Management* **34**, S39–S60 (2004)
 19. Host, G.E., Polzer, P.L., Mladenoff, D.J., White, M.A., Crow, T.R.: A quantitative approach to developing regional ecosystem classifications. *Ecological Applications* **6**, 608–618 (1996)
 20. Iyigun, C., Türkeş, M., Batmaz, İ., Yozgatligil, C., Purutcuoğlu, V., Koç, E.K., Öztürk, M.Z.: Clustering current climate regions of turkey by using a multivariate statistical method. *Theoretical and applied climatology* **114**(1-2), 95–106 (2013)
 21. Jain, A.K., Dubes, R.C.: *Algorithms for Clustering Data*. Prentice-Hall, Inc. (1988)
 22. Jain, A.K., Murty, M.N., Flynn, P.J.: Data clustering: A review. *ACM Computing Surveys* **31**(3), 264–323 (1999)
 23. Kamvar, S.D., Klein, D., Manning, C.D.: Spectral learning. In: *IJCAI*, pp. 561–566 (2003)
 24. Kondor, R.I., Lafferty, J.D.: Diffusion kernels on graphs and other discrete input spaces. In: *19th Int'l Conference on Machine Learning*, pp. 315–322. Morgan Kaufmann Publishers Inc. (2002)
 25. Kreft, H., Jetz, W.: A framework for delineating biogeographical regions based on species distributions. *Journal of Biogeography* **37**, 2029–2053 (2010)
 26. Legendre, P., Legendre, L.: *Numerical ecology*. Amsterdam (2012)
 27. Li, Y., Shi, Z., Li, F., Li, H.Y.: Delineation of site-specific management zones using fuzzy clustering analysis in a coastal saline land. *Computers and Electronics in Agriculture* **56**, 174–186 (2007)
 28. Long, J.A., Nelson, T.A., Wulder, M.A.: Regionalization of landscape pattern indices using multivariate cluster analysis (2010)
 29. von Luxburg, U.: A tutorial on spectral clustering. *Statistics and Computing* **17**(4), 395–416 (2007)
 30. Margules, C.R., Faith, D.P., Belbin, L.: An adjacency constraint in agglomerative hierarchical classifications of geographic data. *Environment and Planning A* **17**(3), 397–412 (1985)
 31. McMahon, G., Gregonis, S., Waltman, S., Omernik, J., Thorson, T., Freeouf, J., Rorick, A., Keys, J.: Developing a spatial framework of common ecological regions for the conterminous united states. *Environmental Management* **28**(3), 293–316 (2001)
 32. Miele, V., Picard, F., Dray, S.: Spatially constrained clustering on ecological networks. *Methods in Ecology Evolution* **5**(8), 771–779 (2014)
 33. Murtagh, F.: A survey of algorithms for contiguity-constrained clustering and related problems. *The Computer Journal* **28**(1), 82–88 (1985)
 34. Omernik, J.M.: Ecoregions: A spatial framework for environmental management. In: W.S. Davis, T.P. Simon (eds.) *Biological assessment and criteria: tools for water resource planning and decision making*, pp. 49–62. Lewis Publishers, Boca Raton, Florida (1995)
 35. Openshaw, S.: A regionalisation program for large data sets. *Computer Applications* **136**, 47 (1973)
 36. Rand, W.: Objective criteria for the evaluation of clustering methods. *Journal of the American Statistical Association* **66**(336), 846–850 (1971)
 37. Rao, A.R., Srivnivas, V.: Some problems in regionalization of watersheds. *Water Resources Systems -Water Availability and Global Change* **280**, 301–308 (2003)
 38. Recchia, A.: Contiguity-constrained hierarchical agglomerative clustering using sas. *Journal of Statistical Software* **33**, 1–12 (2010)
 39. Sandin, L., Johnson, R.K.: Ecoregions and benthic macroinvertebrate assemblages of swedish streams. *Journal of the North American Benthological Society* **19**, 462–474 (2000)

40. Savaresi, S.M., Boley, D.L.: A comparative analysis on the bisecting k-means and the PDDP clustering algorithms. *Intelligent Data Analysis* **8**(4), 345–362 (2004)
41. Seaber, P.R., Kapinos, F., Knapp, G.L.: Hydrologic unit maps. U.S. Geological survey water-supply papers (1987)
42. Shi, J., Malik, J.: Normalized cuts and image segmentation. *IEEE Transactions on Pattern Analysis and Machine Intelligence* **22**(8), 888–905 (1997)
43. Shi, X., Fan, W., Yu, P.S.: Efficient semi-supervised spectral co-clustering with constraints. In: *Proc of IEEE Int'l Conf on Data Mining*, pp. 1043–1048. IEEE Computer Society (2010)
44. Sneath, P., Sokal, R.: *Numerical taxonomy wh freeman and company san francisco* (1973)
45. Sokal, R.R.: A statistical method for evaluating systematic relationships. *Univ Kans Sci Bull* **38**, 1409–1438 (1958)
46. Soranno, P., et al.: Building a multi-scaled geospatial temporal ecology database from disparate data sources: Fostering open science through data reuse. *Journal of Giga Science* (2015)
47. Soranno, P., et al.: Lagos-ne: a multi-scaled geospatial and temporal database of lake ecological context and water quality for thousands of us lakes. *GigaScience* **6** (2017)
48. Sørensen, T.: A method of establishing groups of equal amplitude in plant sociology based on similarity of species and its application to analyses of the vegetation on danish commons. *Biol. Skr.* **5**, 1–34 (1948)
49. Tan, P.N., Steinbach, M., Kumar, V.: *Introduction to data mining, (First Edition)*. Addison-Wesley Longman Publishing Co., Inc. (2005)
50. Wagstaff, K., Cardie, C., Rogers, S., Schroedl, S.: Constrained k-means clustering with background knowledge. In: *Proc of IEEE Int'l Conf on Machine Learning*, pp. 577–584. Morgan Kaufmann (2001)
51. Wang, X., Davidson, I.: Flexible constrained spectral clustering. In: *16th ACM SIGKDD International Conference on Knowledge Discovery and Data Mining*, pp. 563–572. ACM (2010)
52. Ward Jr, J.H.: Hierarchical grouping to optimize an objective function. *Journal of the American statistical association* **58**, 236–244 (1963)
53. Wolock, D.M., Winter, T.C., McMahon, G.: Delineation and evaluation of hydrologic-landscape regions in the united states using geographic information system tools and multivariate statistical analyses. *Environmental Management* **34**, S71–S88 (2004)
54. Wu, J.: Hierarchy theory: An overview. *Linking Ecology and Ethics for a Changing World* **1**, 281–301 (2013)
55. X.Wu, Murray, A.T.: A new approach to quantifying spatial contiguity using graph theory and spatial interaction. *Journal of Geographical Information Science* **22**, 387–407 (2008)
56. Yuan, S., Tan, P., Cheruvilil, K., Collins, S., Soranno, P.: Constrained spectral clustering for regionalization: Exploring the trade-off between spatial contiguity and landscape homogeneity. In: *Proceedings of the IEEE International Conference on Data Science and Advanced Analytics* (2015)